



TSUNAMI HAZARD ASSESSMENT IN SOUTHERN PERU USING NUMERICAL SIMULATION

J. Morales⁽¹⁾, S. Koshimura⁽²⁾, Y. Fujii⁽³⁾, M. Estrada⁽⁴⁾, E. Mas⁽⁵⁾, B. Adriano⁽⁶⁾

⁽¹⁾ Assistant Researcher, Japan Peru Center for Earthquake Engineering Research and Disaster Mitigation, Faculty of Civil Engineering, National University of Engineering, jmoralest@uni.pe

⁽²⁾ Associate Professor, International Research Institute of Disaster Science, Tohoku University, koshimura@irides.tohoku.ac.jp

⁽³⁾ Senior Research Scientist, International Institute of Seismology and Earthquake Engineering, Building Research Institute, fujii@kenken.go.jp

⁽⁴⁾ Director(e), Japan Peru Center for Earthquake Engineering Research and Disaster Mitigation, Faculty of Civil Engineering, National University of Engineering, estrada@uni.edu.pe

⁽⁵⁾ Assistant Professor, International Research Institute of Disaster Science, Tohoku University, mas@irides.tohoku.ac.jp

⁽⁶⁾ Research Student, International Research Institute of Disaster Science, Tohoku University, badrianoo@geoinfo.civil.tohoku.ac.jp

Abstract

Peru is located in high a seismicity region, reason why great tsunamis have occurred, one of them the 1868 Arica tsunami caused massive destruction in the southern Peru and the northern Chile, with an approximately 9.0 moment magnitude (Mw.)

The purpose of this study is to develop tsunami hazard maps in the southern Peru through numerical simulation.

Using as source models, the 1868 tsunami and a possible future event, the tsunami mapping were developed.

The target area in this study is Ilo City in Moquegua Region, which is very prone to tsunami damages, not only because of the existence of a seismic gap, since 1868, but also because of the unawareness of people and the lack of hazard maps in the area.

Numerical simulations were executed using the TUNAMI-N2 code, developed by the Disaster Control Research Center (DCRC), Tohoku University, Japan, with Cartesian coordinates for a nested grid system.

The results of the historical source were compared with those obtained by Okal et al. (2006) showing concordance. Also by using the recorded data available of the wave height reached in cities of Peru and Chile it was possible to validate the model.

The maximum inundation height was up to 14 m for the historical event and could cause serious damage and even worse could stop the economic activities of the area. For the future event there is not much inundation but the high velocities should be taken into account.

The results obtained in this study may help to understand the tsunami inundation features in southern Peru, increasing the awareness through hazard maps and possible evacuation routes.

Keywords: 1868 Earthquake; Ilo City, hazard map, tsunami inundation.

1. Introduction

The high seismicity around Peru comes mainly from the interaction between the Nazca Plate and the South American Plate, as a result Peru has experienced numerous large earthquakes in its history. The western edge of Peru is located inside the boundary known as the “Ring of Fire”, the most seismically active region in the world.

Studies of the source areas of major historical tsunamis in this region show that the earthquakes tend to line up along the Peru-Chile trench [1].

This study will focus on the 1868 Arica earthquake and tsunami. Due to them having occurred over a century ago, information is limited. However, it is known that on August 13th, 1868 an earthquake of approximately Mw 9.0 struck the south of Peru, affecting the cities of Arequipa, Moquegua, Tacna, Arica and Iquique (these last two cities are now in Chile). A huge tsunami followed, in which the first wave to hit Arica, 12 m in height, arrived 52 minutes after the earthquake and a second wave of 16 m arrived 73 minutes after that [2]. Due to both, the earthquake and tsunami, there were more than 25,000 casualties according to the National Geophysical Data Center (NGDC). The agitation of the ocean reached as far as California, Hawaii, Yokohama, the Philippines, Sydney and New Zealand [3].

There has been 148 years since the Arica earthquake and tsunami and seismological studies confirm the existence of a seismic gap in the area [4], reason why the purpose of this study is to determine tsunami inundation maps along one of the more populated coastal cities, Ilo City, using three different source scenarios, two historical and one future, through numerical modeling. Additionally there will be results of maximum wave velocities.

2. Theoretical Background

2.1 Shallow Water theory

In the shallow water theory, there is an assumption that water depth is much shallower than the horizontal component of the wavelength. The continuous non-linear two-dimensional shallow water equations, Eq. (1), Eq. (2) and Eq. (3) are discretized by the staggered leapfrog finite difference scheme [5] using a constant grid size for each region with Cartesian coordinates. The final two basic expressions of the shallow water theory are shown below.

The continuity equation can be written as:

$$\frac{\partial \eta}{\partial t} + \frac{\partial M}{\partial x} + \frac{\partial N}{\partial y} = 0 \quad (1)$$

where, η is the wave amplitude, M and N are the discharge fluxes in the x and y direction and t is the time.

The momentum equations with bottom friction terms can be written as:

$$\frac{\partial M}{\partial t} + \frac{\partial}{\partial x} \left(\frac{M^2}{D} \right) + \frac{\partial}{\partial y} \left(\frac{MN}{D} \right) = -gD \frac{\partial \eta}{\partial x} - \frac{gn^2}{D^{7/3}} M \sqrt{M^2 + N^2} \quad (2)$$

$$\frac{\partial N}{\partial t} + \frac{\partial}{\partial x} \left(\frac{MN}{D} \right) + \frac{\partial}{\partial y} \left(\frac{N^2}{D} \right) = -gD \frac{\partial \eta}{\partial y} - \frac{gn^2}{D^{7/3}} N \sqrt{M^2 + N^2} \quad (3)$$

where, D is the total water depth ($D=\eta+h$), n is the Manning roughness coefficient, g is the gravitational acceleration and h is the sea depth.

2.2 Seafloor Deformation

Sea surface deformation is assumed at the instant of seismic deformation of the sea floor, so the features of the sea bottom deformation reflect the initial water surface elevation and assumed to be the initial condition of the tsunami simulation. This initial condition is calculated by using the equations of Okada [6] derived from Green's function solution to the elastic half space problem.

2.3 Tsunami Propagation and Inundation

The simulation was performed using the TUNAMI-N2 (Tohoku University's Numerical Analysis Model for Investigation of Near-field Tsunami No.2) code based on shallow water theory, which was developed by the Disaster Control Research Center (DCRC) of Tohoku University, Japan.

Propagation and inundation were calculated by using the TUNAMI-N2 code in a Cartesian coordinate system. The computational area was divided into four and three domains for historical and future events respectively and each domain was connected by using a nested grid system (Fig. 1).

3. Data

3.1 Bathymetry and Topography data

The bathymetry data was interpolated from the General Bathymetry Chart of the Ocean (GEBCO) 30 arc-seconds grid data for the largest domains, and for the smallest domain the bathymetry was generated from the nautical chart of the Directorate of Hydrography and Navigation (DHN), data interpolated up to 30 meters.

For the topography data only in the smallest domain we used the data from the Thermal Emission and Reflection Radiometer (ASTER), 1 arc-second resolution instead of GEBCO.

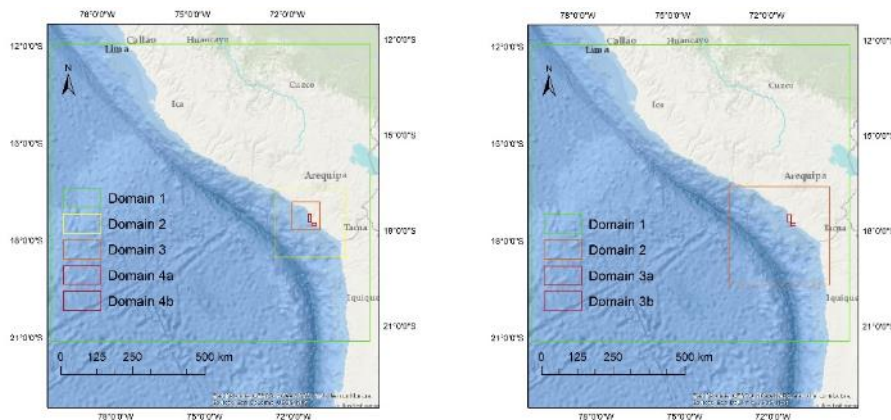


Fig. 1 - Domains used in this study for historical event (left) and future event (right).

The following Table 1 and Table 2 show the minimum and maximum coordinates, the grid resolution and the data source used for each domain of the historical and future event respectively.

Table 1 - Boundaries, resolution and data source for each computational domain for historical event.

Domain	Latitude (deg)		Longitude (deg)		Resolution m	Data Source	
	Min	Max	Min	Max		Bathymetry	Topography
1	-79.99	-69.37	-21.48	-11.95	810	GEBCO 30s	GEBCO 30s
2	-72.51	-70.20	-18.84	-16.62	270	GEBCO 30s	GEBCO 30s

3	-71.95	-71.01	-17.97	-17.09	90	GEBCO 30s	GEBCO 30s
4	-71.40	-71.30	-17.71	-17.47	30	DHN 30m	ASTER 30m

Table 2 - Boundaries, resolution and data source for each computational domain for future event.

Domain	Latitude (deg)		Longitude (deg)		Resolution	Data Source	
	Min	Max	Min	Max	m	Bathymetry	Topography
1	-79.99	-69.37	-21.48	-11.95	270	GEBCO 30s	GEBCO 30s
2	-73.38	-70.04	-19.70	-16.56	90	GEBCO 30s	GEBCO 30s
3	-71.40	-71.30	-17.71	-17.47	30	DHN 30m	ASTER 30m

3.2 Historical Event Sources

For the 1868 Arica earthquake two possible scenarios were selected; the first using only a single fault and the second using two faults [7].

The first source uses only the Fault 1 and has 8.7 Mw, while the second source proposed by Okal uses a second fault northward the first one and has an Mw of 9.0 (Table 3 and Fig. 2).

Table 3 - Parameters of the faults used for Sources 1 and 2.

F.	Lat. (deg)	Lon. (deg)	Slip (m)	Length (km)	Width (km)	Strike (deg)	Dip (deg)	Rake (deg)	Depth (km)	Mw	Mw
1	-18.7	-71.2	15	600	150	305	20	90	20	8.7	9.0
2	-15.9	-75.8	15	300	150	330	20	90	20	8.5	

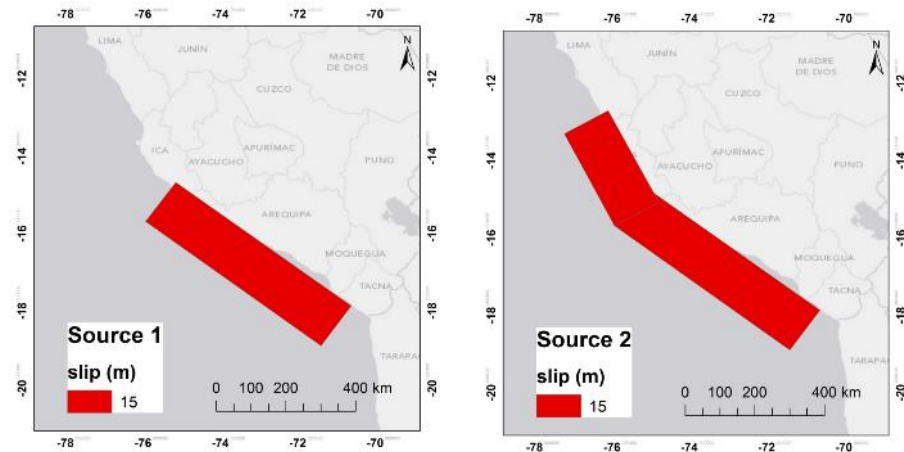


Fig. 2 - Source 1 using a single fault (left), source 2 using both faults (right), See Table 3 for each fault.

3.3 Future Event Source

Twelve slip scenario models were calculated considering slip deficit during an interseismic period from the 1868 earthquake to the present [8].

The models have magnitudes around 8.5 Mw and a source area of 56000 km², 280 km along strike and 200 km along dip, the strike is 313 degrees, the dip is 20 degrees and the average rake angle for all sub-faults is 54.6 degrees. The model also has 28 sub-faults along the strike and 20 along the dip, and the sub-fault size is 10 km x 10 km. Fig. 3 shows one of the slip scenarios.

From the twelve scenarios, the most adverse case was assumed to be the one which displaces most water during the faulting. The steps to find the volume of displaced water were:

- a) To find the seafloor deformation for each slip scenario by using the Okada code [6].
- b) To take the absolute value of the deformation values (height in meters, Fig.2)
- c) To multiply the deformation values (height in meters) obtained, by the area of each cell, in this case it was computed for domain 2, where the cells size are 90 m x 90 m (see Table 2).
- d) Finally, the sum of the values obtained in the previous step is the volume of displaced water.

The results of this calculation are shown in Table 4.

Table 4 - Volume of displaced water for each scenario.

Scenario	Volume of displaced water (10 ¹⁰ m ³)
1	3.943
2	3.884
3	4.375
4	4.134
5	4.382
6	3.798
7	3.692
8	3.736
9	4.033
10	4.087
11	4.447
12	4.196

After comparing the displaced volumes of water for each scenario (Table 4), it was found that in the 11st scenario, 44.47 billion of cubic meters were displaced; the maximum amount between all the scenarios. Thus the simulation was carried out using this source. Fig. 3 shows the slip distribution of the chosen scenario and Fig. 4 shows the calculated seafloor deformation of the scenario 11.

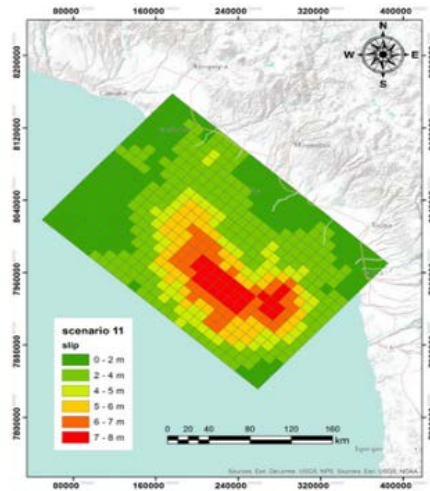


Fig. 3 – Slip distribution of the scenario 11.

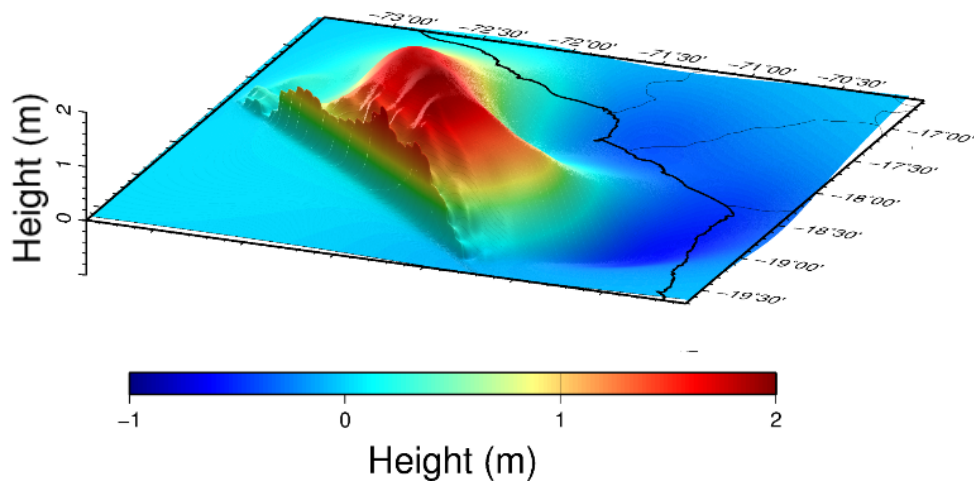


Fig. 4 - Seafloor deformation in scenario 11, chosen to be modeled.

3.4 Historical Data

In order to validate the 1868 event, the values of tsunami height and inundation area were necessary. Due to the age of this event the Tsunami Laboratory catalog of the Institute of Computational Mathematics and Mathematical Geophysics (SB RAS) in Novosibirsk, Russia was used as a reference. Table 5 shows recorded heights and locations for the 1868 Arica tsunami.

Table 5 - Recorded tsunami height and computed results.

Place	Lon (deg)	Lat (deg)	Recorded height (m)	S1 Height (m)	S2 Height (m)
Callao	-77.13	-12.08	4.00	2.15	5.44
Arica	-70.33	-18.48	15.00	12.77	12.73
Chala	-74.22	-15.88	15.00	9.87	9.85
Islay	-72.10	-17.03	12.00	12.14	12.1
Ilo	-71.33	-17.70	10.00	10.87	10.82
Mollendo	-72.00	-17.00	10.00	12.35	10.16

4. Results and Discussion

4.1 Tsunami Propagation

Tsunami propagation was computed using a set of virtual tidal gauges along the coastal area, located every 100 meters, for the historical earthquake. These virtual tidal gauges allowed the estimation of tsunami heights along the Peruvian coast within domain 1 (Fig. 3 and Table 2).

The tsunami height in Pisco city reached no more than 3 meters with source 1, but according to local news reports, the city was totally destroyed, this is why Source 2 was proposed by Okal in 2006 [7]; then adding the second fault creates a tsunami height near to 10 meters, capable of causing the destruction of Pisco.

The Fig. 5 shows the differences between the results by Okal [7] and those from this study, where this differences are mainly due to the fact that this study used finer bathymetry and topography grid data, 810 meter grids in the largest domain, while in Okal's simulation a grid resolution of 2 km was used.

Another significant difference is that the fault's epicenter was found graphically using GIS tools from the Okal's model, because this information was not in their study. Nevertheless the results obtained fit the recorded values in different cities in Peru and Chile, see Table 4.

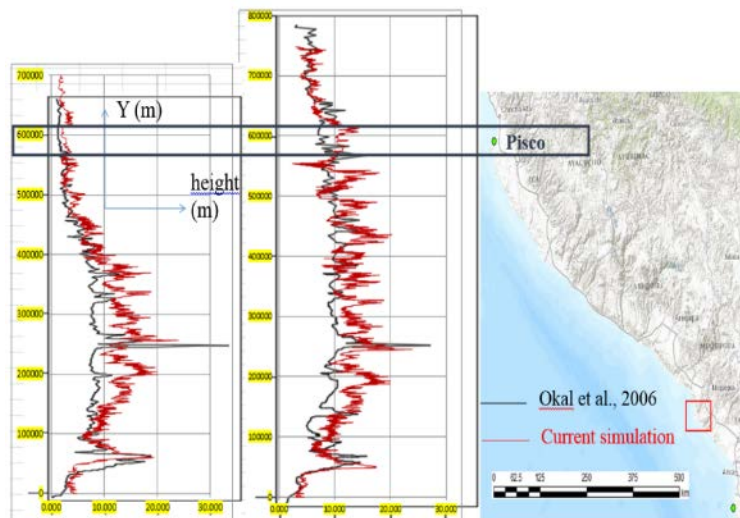


Fig. 5 - Tsunami heights along the coast area, Source 1 (left), Source 2 (right).

4.2 Tsunami Inundation and maximum velocities

4.2.1 Historical event (Sources 1 and 2)

Tsunami inundation was calculated for the domain of greatest resolution for Ilo city, the computation time was 5 hours in each case and the maximum inundation height was 14 meters. The most affected areas were the port of Ilo, some beaches and areas around the Osmore River (Fig. 6). From this map it was found that in case of a tsunami similar to the 1868 event, all the economic activity related to the port would be halted, and some summer resorts would be affected. Fortunately the topography of the whole area is very steep and high, causing the inundation to decrease quickly going inland and, even better, this helps people to reach safe areas in a short time.

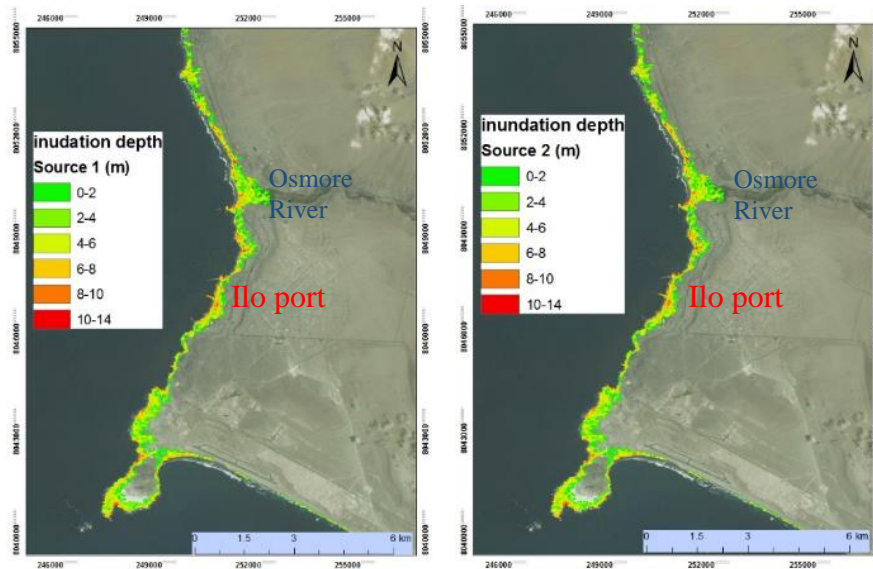


Fig. 6 - Maximum tsunami inundation depth map for Source 1 (left) and Source 2 (right).

The maximum velocities were also calculated (Fig. 7). The results show very high velocity waves reaching up to 16 m/s, but decreasing considerably inland, the average velocities being from 8 to 10 m/s. Due to the main economic activity of the city being dependent on the port, there are dozens of fishing boats, cargo and even mining vessels. The velocities found at the coast around the port reached almost 16 m/s which would cause huge damage not only to the boats but also to the buildings and structures inland that vessels may impact.

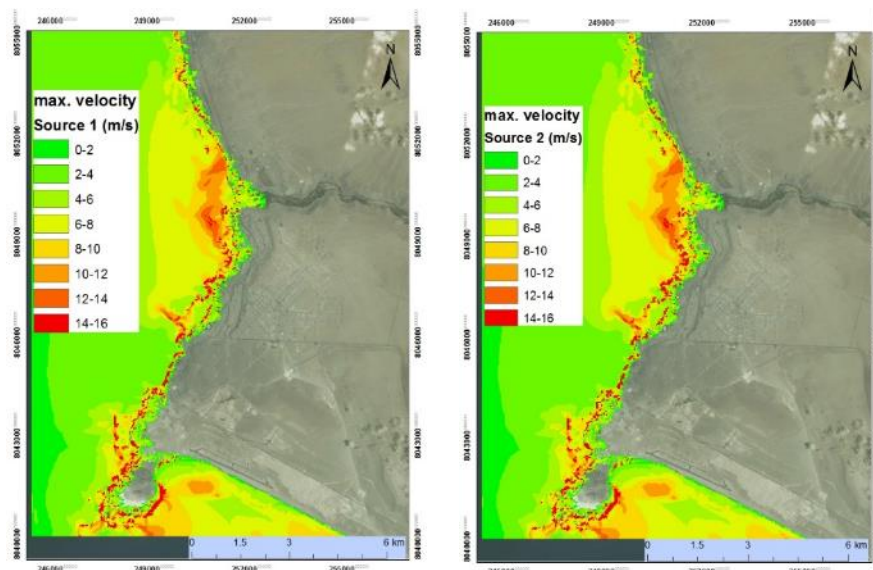


Fig. 7 - Maximum velocities map for Source 1 (left) and Source 2 (right).

4.2.2 Future event (Source 3)

In this case, from twelve available scenarios, only the most adverse case was modeled (Table 4) and the computation time was 5 hours. The computation results show no inundation (Fig. 8) and this is explained by the steep topography in the area.

Even though there is no inundation, again it is important to analyze the flow velocities in order to determine the possible risk around significant locations.

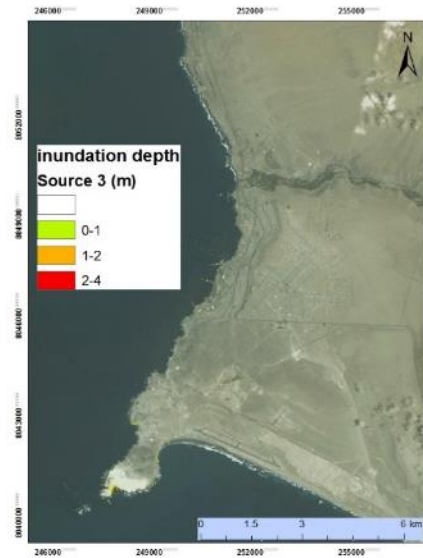


Fig. 8 - Inundation map for Source 3.

On the other hand Fig. 9 shows calculated velocities. The velocities are much less than the ones from Sources 1 or 2, but are still high velocities capable of causing huge damage to vessels or structures along the shoreline, mainly in areas near Ilo port or the summer resorts, places with potentially high populations during the event.

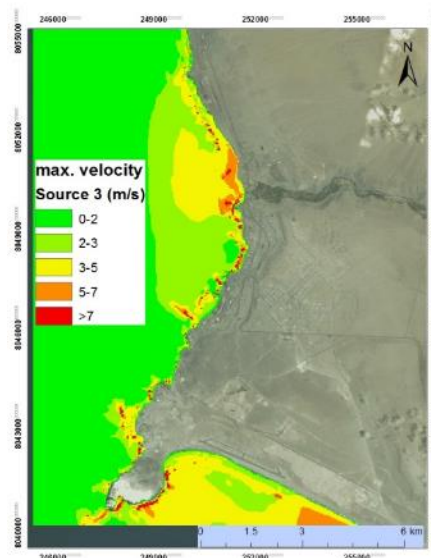


Fig. 9 - Maximum velocities map for Source 3.

5. Conclusions

It was performed tsunami numerical simulations using two different historical sources (Source 1 with Mw 8.7 and Source 2 with Mw 9.0). The computation results were consistent with those of Okal [7], and by using recorded data from the Tsunami Laboratory catalog of the Institute of Computational Mathematics and Mathematical Geophysics (SB RAS) in Novosibirsk, Russia. It was found that the second was more suitable to reproduce the historical records. However this second source crosses the Nazca Ridge and there are few historical earthquakes with a rupture that crosses the ridge. Thus, Source 1 might be more appropriate to develop the hazard maps.

The results obtained from the historical sources indicate inundation depths of up to 14 meters, with the most affected areas potentially being the port of Ilo and summer resorts located along the coast. Furthermore the flow velocities with these models were comparable with velocities in the great 2011 Tohoku tsunami (~10m/s) and would have great destructive power even if the inundation area is not very large.

Using the future event (Source 3 with Mw = 8.5), no inundation was found in the Ilo district. However, the flow velocities are high enough to cause damage to structures and vessels around the shore area.

5. Recommendation

In order to increase the reliability of the tsunami simulation, would be important to carry out the far-field computation and compare the results with recorded values in Hawaii, New Zealand and other locations around the world where it was well known that the water arrived.

Obtaining good bathymetry for the areas of Vila Vila, Boca del Rio and Arica would help to enhance this study by allowing a comparison not only of tsunami heights, but also flow velocities obtained through sedimentology studies.

Even knowing that the velocities in all cases are very high and may cause damage to structures, it is possible to know how resistant a structure would be through coastal engineering for important structures such as Ilo port and the dock of the Enersur power plant located southward the port.

6. References

- [1] Hatori T (1981): Colombia-Peru tsunamis observed along the coast of Japan, 1960-1970, *Bulletin of the Earthquake Research Institute* (in Japanese with English abstract), University of Tokyo, Vol. 56, No. 3, p. 535-546.
- [2] Zamudio Z, Berrocal J, Fernandes C (2005): *Seismic hazard assessment in the Peru-Chile border region*, 6th International Symposium on Andean Geodynamics (ISAG 2005, Barcelona), Extended Abstracts: 813-816.
- [3] Ravinovich A, Kulikov A, Thomson R (2001): *Tsunami Risk Estimation for the Coasts of Peru and Northern Chile*, ITS 2001 Proceedings, Session 1, Number 1-5.
- [4] Chlieh M, Perfettini H, Tavera H, Avouac J, Remy D, Nocquet J, Rolandone F, Bondoux F, Gabalda G, Bonvalot S (2011): *Interseismic Coupling and Seismic Potential along the Central Andes Subduction Zone*, *J. Geophys. Res.*, 116, B12405, doi: 10.1029/2010JB008166.
- [5] Iamura F (1995): Review of the Tsunami Simulation with a Finite Difference Method, Long Wave Run-up Models, *World Science*, 25-42.
- [6] Okada Y (1985): Surface Deformation Due to shear and Tensile Faults in Half-space, *Bulletin Seismological Society of America*. Vol. 75, No. 4, 1135-1154.
- [7] Okal E, Borrero J, Synolakis C (2006): Evaluation of Tsunami Risk from Regional earthquakes at Pisco, Peru, *Bulletin of the Seismological Society of America*, Vol. 96, No 5, pp. 1634-1648, doi: 10.1785/0120050158.
- [8] Pulido N, Nakai S, Yamanaka H, Calderon D, Aguilar Z, Sekiguchi T (2014): Estimation of a Source Model Strong Motion Simulation for Tacna City, South Peru, *Journal of Disaster Research*, Vol. 9 No.6.